

Wave Energy Potential in the Mediterranean and Black Seas: A 15-Year Hindcast and Ocean Current Influence

John Karagiorgos^{1[0000-0003-2451-8931]}, Rushit Dallenga^{1[0009-0008-1213-2592]},
Vassilios Vervatis^{1[0000-0002-8862-8155]}, and Sarantis Sofianos^{1[0000-0001-6325-513X]}

¹Department of Physics, Section of Environmental Physics & Meteorology
National and Kapodistrian University of Athens, 15784 Athens, Greece
j.karagiorgos@phys.uoa.gr

Abstract. The growing energy demand has intensified interest in marine renewable sources. This study assesses wave energy potential in the Mediterranean and Black Seas using a 15-year (2010–2024) wave hindcast with the WaveWatch III model. It examines the spatial and temporal distribution of significant wave height, wave energy period, and overall wave energy resources at a basin-wide scale. The findings identify the western Mediterranean—particularly the area west of Sardinia and from the Gulf of Lion to the Algerian coast—as having considerable wave energy potential, primarily due to the Mistral winds during winter. Other regions, such as the Alboran Sea, central-south Aegean Sea, and western Black Sea, show lower wave energy levels but remain promising for the deployment of wave energy converters (WECs) due to moderate wave power variability over time. To assess the impact of wave-current interactions on wave power estimation, additional simulations were performed over a 5-year sub-period without current forcing. Results indicate that currents can reduce extreme wave power values in the most energetic areas by up to 5 kW m^{-1} . This study establishes a baseline wave-only simulation to aid future research using a regional coupled ocean-atmosphere-wave system for more precise wave power assessments.

Keywords: renewable energy sources, offshore wave energy, numerical modeling, WaveWatch III, wave-current interactions, Mediterranean Sea, Black Sea.

1 Introduction

The escalating concerns about climate change and the environmental impact of fossil fuels have intensified the search for renewable energy sources capable of generating electricity with negligible carbon dioxide emissions [1]. Among these sources, ocean energy, particularly from ocean waves, has gained attention as a promising and abundant alternative [2,3]. However, wave energy converters (WECs) are still in the early stages of development and face significant challenges, including limited lifespans and high construction and maintenance costs due to the harsh marine environment [4]. Despite these obstacles, refined wave resource assessment and characterization of sea

states are crucial for identifying suitable locations for energy extraction and optimizing WECs design to match environmental conditions and available power [5].

The Mediterranean and Black Seas are interconnected semi-enclosed basins where complex morphology and shallow coastal regions constrain fetch length, thereby shaping wave dynamics and affecting wave power potential. The waves in these environments are short-crested and highly influenced by local wind dynamics and seasonal variability. Despite these constraints, certain areas exhibit promising wave energy potential, making them valuable for renewable energy exploration (e.g., [6,7]). Various studies have investigated wave energy resources, primarily in the Mediterranean, at both the basin scale (e.g., [8-14]) and in specific regions (e.g., [15-21]). Additionally, other studies have explored the potential for the joint exploitation of wind and wave energy resources (e.g., [22-25]). In the context of climate change impacts on sea state conditions, recent studies have focused on wave energy patterns under different climate scenarios (e.g., [26-29]).

Numerical simulation is a key tool in energy resource assessment, offering critical insights into the selection of wind and wave farm locations and their operational management. Several studies (e.g., [30-32]) highlight the importance of including ocean currents in wave models, as they have an impact on the wave spectrum and, consequently, the estimated wave power. Wu [33] emphasized the importance of atmosphere-ocean-wave interactions in improving wind and wave energy potential estimates. In the domain of interest, research on current-induced effects on wave power estimation remains limited (e.g., [34,35]), making this study a valuable contribution.

Within the broader context of assessing marine renewable resources and their efficient exploitation, this study explores the variability of offshore wave energy potential in the Mediterranean and Black Seas through a wave hindcast simulation for the recent past (2010–2024). It also presents a quantitative evaluation of how the ocean current forcing affects wave spectral parameters and, in turn, the wave energy potential estimation on a basin-wide scale. This paper is organized as follows: Section 2 provides a description and evaluation of the numerical model used, followed by the methodology for assessing wave energy potential. Section 3 presents the main results for the two sub-basins, including a discussion on the spatio-temporal distributions of wave power and the effect of currents. Section 4 provides a summary of this work and future directions.

2 Methodology

2.1 Wave hindcast

The sea wave conditions analyzed in this paper are based on a 15-year hindcast (2010–2024) using the WaveWatch III (WW3 v6.07; [36]) wave model for the interconnected Mediterranean-Black Sea system (Fig. 1). WW3 is a third-generation spectral wave model that solves the two-dimensional (frequency–direction) wave energy spectrum over time and space. Its application in wave climatology assessments within the study region (e.g., [37,38]) underscores its robustness and reliability. The WW3 configuration utilized here was adapted from the wave component of the coupled mod-

elling system described by Karagiorgos [39]. The model was run on a structured curvilinear grid with a horizontal resolution of $1/12^\circ$ (~ 8 km), and we used a maximum global integration time step of 720 s, CFL time step of 240 s, refraction time step of 360 s, and minimum source term time step of 10 s. The spectral space was discretized using 24 directions ($\Delta\theta=15^\circ$) and 32 frequencies ranging from 0.04118 Hz to 0.79042 Hz (corresponding to wave periods of approximately 1 s to 24 s). The frequency bins were incremented using a step factor of 1.1, such that $f_{n+1}=1.1f_n$, where f_n is the n -th frequency. Further details about the model setup and key parameterizations are detailed by Karagiorgos [39] (see their Appendix A).

The WW3 was forced with 10-m wind field components obtained from the hourly ERA5 reanalysis dataset [40] on a 0.25° spatial grid (Fig. 1a). Additionally, daily-averaged sea surface currents from the GLORYS12 ocean reanalysis [41], with a horizontal resolution of $1/12^\circ$, were used to account for wave-current interactions (Fig. 1b). The currents affect the wave field in two ways: first, the wind input is modified by the current vector, and second, the current field modifies the wave action balance equation through advection, refraction, and Doppler shifting. It is worth noting that the GLORYS12 product is also produced using ERA5 wind forcing at hourly frequency. To assess the impact of ocean currents on wave modeling and wave power potential estimation, an additional WW3 simulation was conducted without current forcing for a 5-year period (2020–2024).

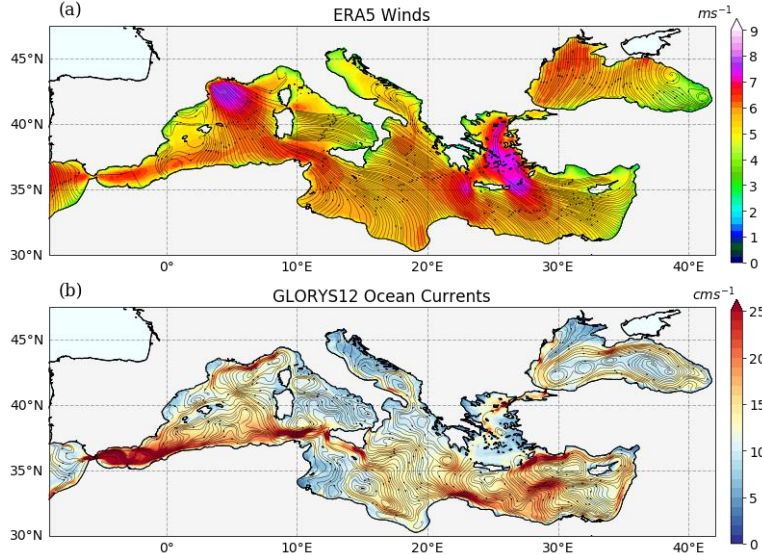


Fig. 1. Integration domain and external forcing for the WW3 wave model: (a) Annual mean wind speed ($m s^{-1}$) from ERA5 and (b) sea surface currents ($cm s^{-1}$) from the GLORYS12 reanalysis over the reference period 2010–2024

2.2 Model evaluation

The WW3 hindcast was evaluated using multi-platform satellite altimeter data distributed by Copernicus Marine Environment and Monitoring Service [42]. Data from ten satellite missions (Jason-3, Sentinel-3A/3B/6A, Cryosat-2, SARAL/AltiKa, CFOSAT, Hai Yang-2B/2C, and SWOT nadir) spanning 2021–2024 were used to assess the ERA5 10-m wind speed (U_{10}), which served as the forcing for WW3, as well as the simulated significant wave height (H_s). The evaluation considered approximately 3.46×10^6 collocations in the Mediterranean and around 6.5×10^5 in the Black Sea. The assessment relied on statistical indicators, including model-minus-observation bias, root mean square error (RMSE), correlation coefficient (R), and the slope of the best-fit line from linear regression.

As shown in Fig. 2a-b, ERA5 wind speeds are slightly underestimated in both basins compared to altimeter measurements, with mean biases of -0.27 m s^{-1} in the Mediterranean and -0.14 m s^{-1} in the Black Sea. The RMSE values are slightly above 1.5 m s^{-1} in both basins, while the correlation coefficients are 0.84 for the Mediterranean and 0.81 for the Black Sea. As a consequence, the simulated H_s is underestimated (Fig. 2c-d), with bias (RMSE) values of -0.3 m (0.41 m) in the Mediterranean and -0.26 m (0.38 m) in the Black Sea. These biases (up to 18%) are primarily due to high H_s values (above 2.5 m), which also reduce the best-fit slope from linear regression (blue line in Fig. 2c-d). However, the correlation coefficient remains high, with a value above 0.9 in both basins. In summary, the simulated significant wave height closely matches satellite observations, strengthening confidence in the model as a reliable tool for conducting wave power assessment in the target regions.

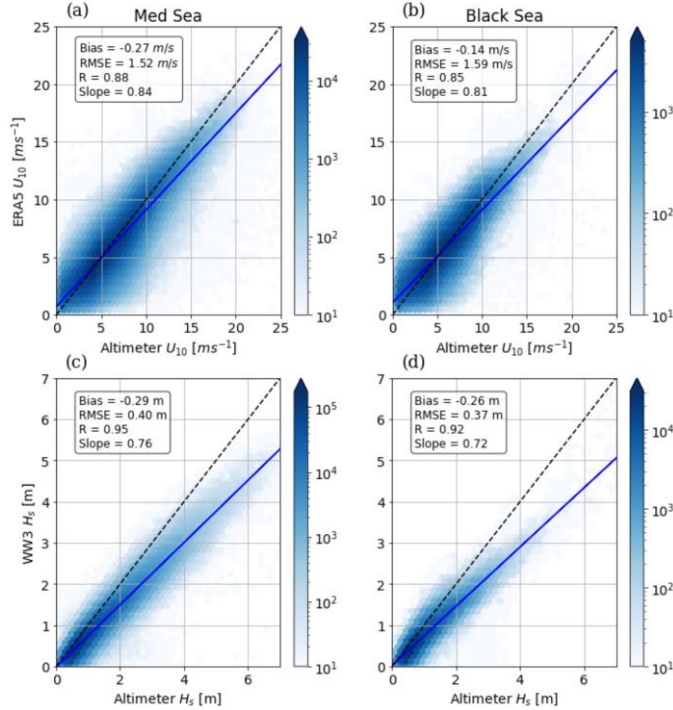


Fig. 2. Scatter plots comparing ERA5 forcing wind speed (U_{10}) and WW3 significant wave height (H_s) with multi-mission altimeter data (L3) over (a, c) the Mediterranean Sea and (b, d) the Black Sea for a 4-year period (2021–2024). The black dashed line represents the best-fit line, while the blue solid line indicates the slope of the least-squares fit

2.3 Wave power computation and variability metrics

The available wave power potential (P_w) expressed in kilowatts per meter of wave crest length (kW m^{-1}) can be calculated using the spectral output of the wave model as:

$$P_w = \rho g \int_0^{2\pi} \int_0^{\infty} c_g(f, h) E(f, \theta) df d\theta \quad [\text{W m}^{-1}] \quad (1)$$

where ρ is the seawater density ($\sim 1025 \text{ kg m}^{-3}$), g is the acceleration due to gravity ($\sim 9.81 \text{ m s}^{-2}$), C_g is the group velocity depending on the local water depth (h) and frequency (f), and E represents the wave energy density distributed across intrinsic frequencies f and propagation directions θ .

For this study, which focuses on offshore regions, Eq. (1) can be simplified using the deep-water approximation:

$$P_w = \frac{\rho g^2}{64\pi} H_s^2 T_p \simeq 0.491 H_s^2 T_p \quad [\text{kW m}^{-1}] \quad (2)$$

where H_s is the significant wave height (m), and T_e is the wave energy period (s), defined as the ratio of the -1st order moment to the 0th order moment of the wave energy density spectrum. Our analysis is based on hourly WW3 outputs for H_s and T_e .

To analyze the temporal variability of wave power (P_w), two metrics were used: the coefficient of variation (CoV) and the monthly variability index (MVI) [43]. The CoV measures the relative variability of wave power in relation to its average value. It is calculated as:

$$CoV = \frac{\sigma_{p_w}}{P_{w,mean}} \quad (3)$$

where σ_{p_w} is the standard deviation of the mean wave power $P_{w,mean}$ over the whole study period. A CoV of 0 indicates no variability, while higher values signify greater variability. The second metric, the monthly variability index (MVI), quantifies the fluctuation of wave power on a monthly scale. It is given by:

$$MVI = \frac{P_{M,max} - P_{M,min}}{P_{w,mean}} \quad (4)$$

where $P_{M,max}$ and $P_{M,min}$ represent the mean wave power during the most and least energetic month, respectively.

3 Results

3.1 Annual and seasonal variability of wave conditions

The offshore mean wave power potential (P_w) in the Mediterranean and Black Seas is closely linked to the spatial variability of wave conditions, in terms of significant wave height (H_s) and mean wave period (T_e). Fig. 3 presents the annual mean distributions of H_s , T_e , and P_w values averaged over the period 2010-2024. The highest wave power levels (above 7 kW m^{-1}) are concentrated in the western Mediterranean (Fig. 3c), particularly west of Sardinia, from the Gulf of Lion to the northern Algerian coasts, where strong winds such as the Mistral generate elevated H_s (above 1 m) and long T_e (~ 5 s) (Fig. 3a-b). The southern Ionian and western Levantine (south of Crete) basins also exhibit intermediate wave energy potential, primarily due to the north-westerly Etesian winds during summer. The Black Sea shows generally lower wave power potential (up to 4 kW m^{-1}), with the western basin ($H_s: \sim 0.8$ m, $T_e: \sim 4$ s) experiencing higher energy levels due to more frequent storms. These spatial patterns reflect the influence of regional atmospheric forcing in shaping sea state and wave energy availability [37].

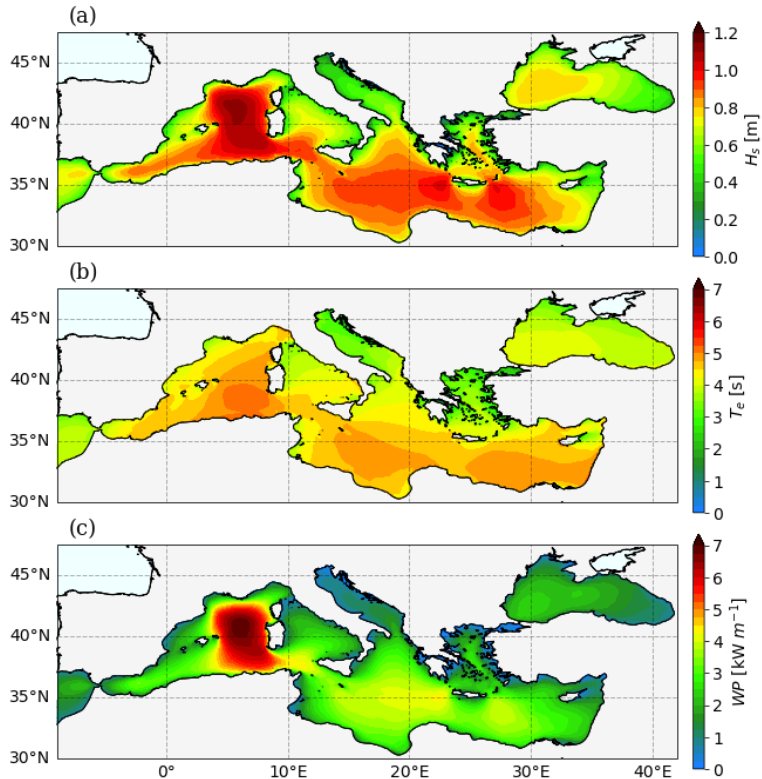


Fig. 3. The average (a) significant wave height (m), (b) mean wave period (s), and (c) wave power potential (kW m^{-1}) over the period 2010-2024

The Mediterranean and Black Seas exhibit pronounced seasonal variability in wave spectral parameters and wave power potential, as illustrated in Figs. 4-6. Frequent storms during winter (DJF) drive the highest H_s (Mediterranean: up to ~ 1.6 m, Black Sea: ~ 1 m) and longest T_e (Mediterranean: ~ 5 –6 s, Black Sea: ~ 4 –5 s), leading to peak wave energy potential above 12 kW m^{-1} (Figs. 4-6a). This is most pronounced in the northwestern Mediterranean influenced by the persistent Mistral, the southern Ionian Sea, the western Levantine, and the western Black Sea. In contrast, summer (JJA) presents the calmest conditions, with the lowest H_s (~ 0.2 –0.8 m) and shortest T_e (~ 3 –5 s), minimizing wave energy potential (Figs. 4-6c). However, localized wave activity persists in the Aegean and Levantine basins, particularly southeast of Crete, where the strong, jet-like Etesian winds sustain higher waves and moderate wave energy levels. The transition seasons reflect intermediate conditions in both basins: in spring (MAM), weakening winds lead to a gradual decrease in H_s (~ 0.6 –1.2 m) and T_e (~ 3 –5 s), reducing wave energy (Figs. 4-6b), while in autumn (SON), increasing storm frequency progressively raises wave activity, particularly in the western and central Mediterranean and the Black Sea, signaling the shift toward winter's higher energy conditions (Figs. 4-6d). Overall, winter's intense wave activity predominantly shapes the annual mean

distribution, while summer and the transition seasons modulate the overall variability across the basins.

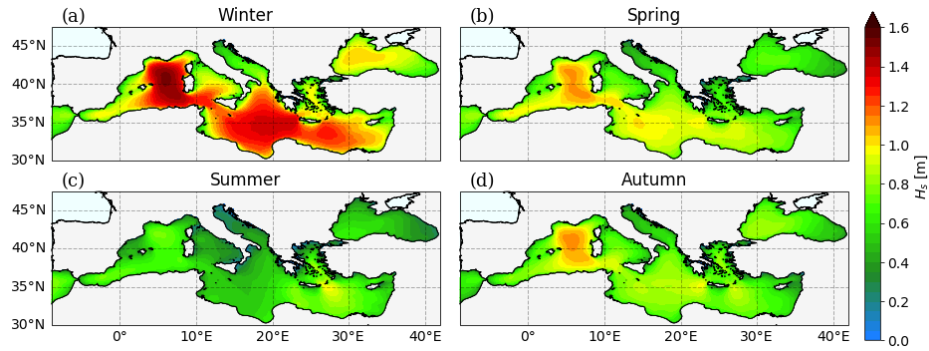


Fig. 4. Seasonal mean significant wave height (m) for 2010–2024: (a) winter (DJF), (b) spring (MAM), (c) summer (JJA), and (d) autumn (SON)

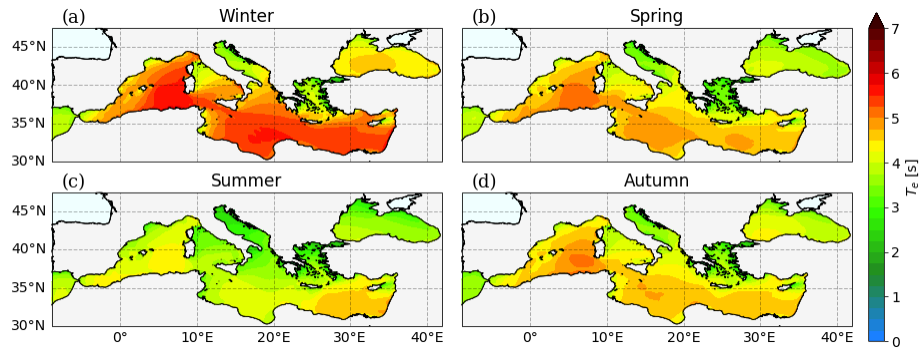


Fig. 5. As in Fig. 4, but for the mean wave period (s)

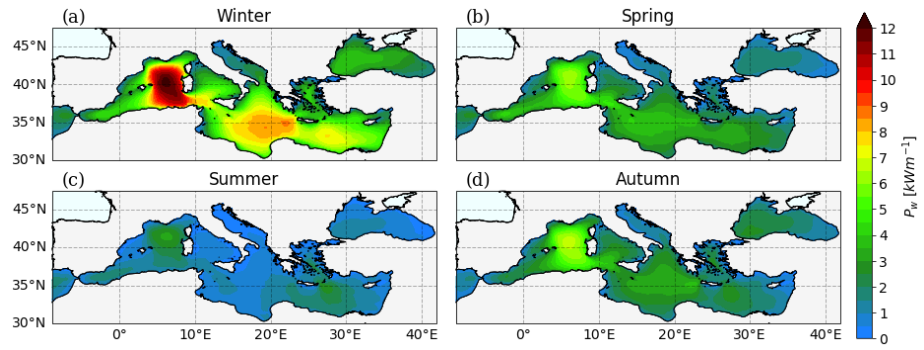


Fig. 6. As in Fig. 4, but for the mean wave power potential (kW m^{-1})

3.2 Wave energy variability metrics

Temporal variability in wave power is a crucial factor for WECs deployment. A region with steady, moderate wave power may be more suitable for installing WECs than an area with high mean wave power but significant temporal variability. To assess both inter-annual and monthly variability, Fig. 7 presents the coefficient of variation (*CoV*) of wave power potential, along with the monthly variability index (*MVI*) over the entire hindcast period (2010–2024). In the Mediterranean, the highest *CoV* indexes are presented at nearshore regions, particularly near the Italian and Greek coastlines and east of Cyprus, where *CoV* exceeds 3 (Fig. 7a), indicating significant variability in wave energy resources. In contrast, the southern and eastern Mediterranean experience relatively lower variability, with *CoV* values around 2. The Alboran Sea, Gulf of Lion, Gulf of Gabes, Aegean Sea, and eastern Libyan coasts display the lowest *CoV* values (~1–1.5), suggesting more stable wave power conditions. In the Black Sea, lower *CoV* values are observed in the northwestern basin, particularly near the Romanian coast and Crimea Peninsula (*CoV*~2), while the southeastern Black Sea experiences greater variability.

The monthly variability of wave power is notably high in the central Mediterranean and the eastern Levantine (*MVI*~2–2.5) (Fig. 7b). In contrast, more sheltered regions, including the Alboran Sea, Gulf of Gabes, Adriatic Sea, and central-southern Aegean Sea, experience relatively stable wave power potential (*MVI*~0.5–1). In the Black Sea, wave resources exhibit relatively low variability on a basin-wide scale, particularly along the southern coasts (*MVI*~1). Overall, areas with low values in both the *CoV* and *MVI* indexes—such as the Alboran Sea, central-southern Aegean Sea, eastern Libyan coasts, and western Black Sea—appear promising for WECs deployment, despite its moderate mean wave power.

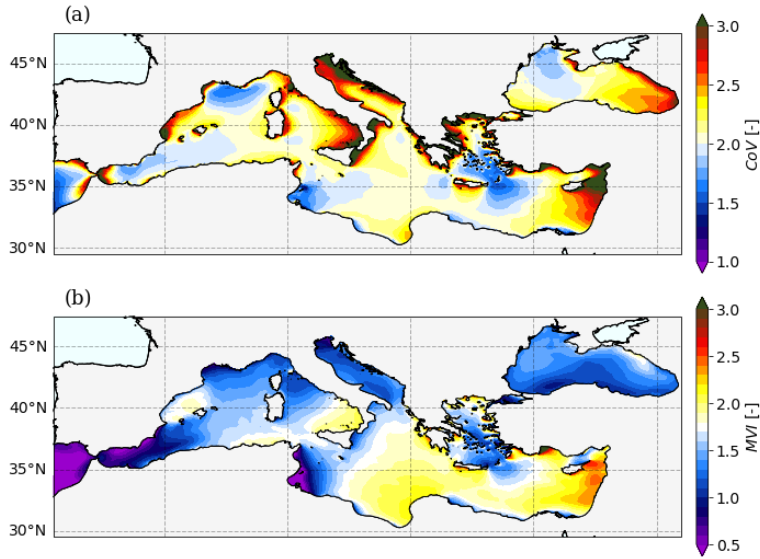


Fig. 7. Spatial distribution of (a) the coefficient of variation (CoV) and (b) the monthly variability index (MVI) of wave power for the reference period: 2010-2024

3.3 Effects of currents on wave power estimations

The inclusion of currents in the wave simulations has influenced wave spectral parameters in both coastal and open-sea regions in the Mediterranean and Black Seas (Fig. 8). On a basin-wide scale, wave energy potential generally decreases (locally by up to ~20% in the Mediterranean and ~27% in the Black Sea), particularly in regions with strong currents (see Fig. 1b and Fig. 8c). However, in certain coastal areas of the western Mediterranean—such as near the Strait of Gibraltar, the northern Gulf of Lion, the Tyrrhenian Sea, and the Adriatic Sea—currents contribute to an increase in wave power potential. Similarly, in the eastern Mediterranean, wave power potential increases north of Cyprus and on certain eastern coasts of the Levantine Sea, as well as along the southern coast of Crete (by up to ~18%). In the Black Sea, currents slightly increase the wave power potential in the eastern coasts of the basin. The main patterns in either the reduction or increase of wave power potential are strongly related to the influence of surface currents on significant wave height and wave period (Fig. 8a-b). For instance, as noted by Benetazzo [46], the opposite or following propagation between waves and currents leads to decrease or increase in wave energy.

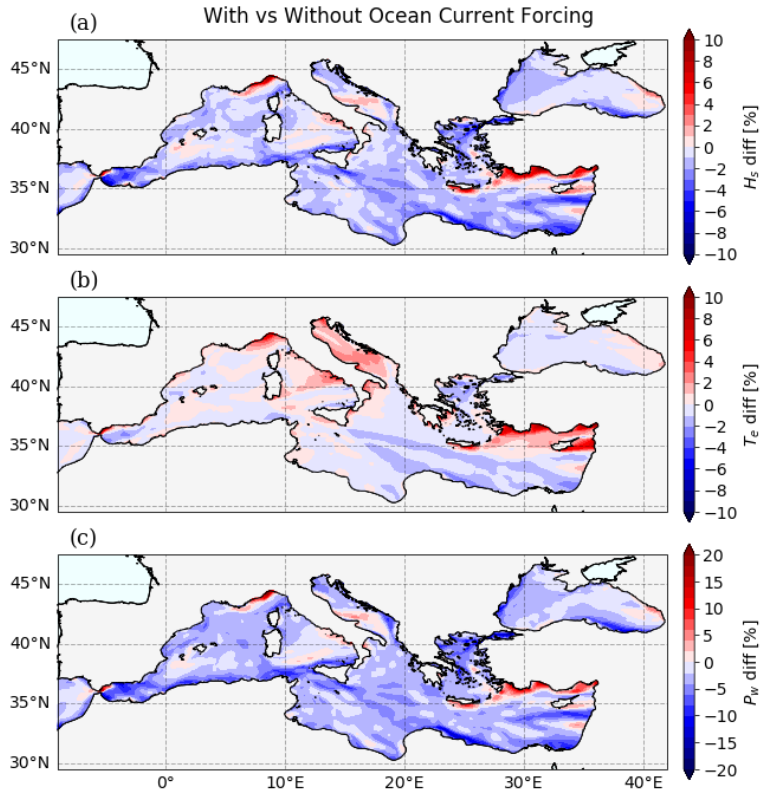


Fig. 8. Percentage of difference in (a) significant wave height, (b) mean wave period, and (c) wave power potential between simulations with and without ocean current forcing for the period 2020–2024

WECs are vulnerable to storm damage, making it vital to consider extreme wave conditions in their placement. Fig. 9 shows the 99th percentile wave power distribution without current forcing, along with the differences between simulations (i.e., with currents minus without currents) over a 5-year period (2020–2024). The highest wave power values are observed in open sea areas (Fig. 9a), with spatial patterns closely resembling those seen under average conditions (see Fig. 3c). Ocean currents generally diminish extreme wave power in the western Mediterranean, reducing it by up to 5 kW m^{-1} , especially along the Algerian coast, west of Sardinia, the Sicily Strait, and the eastern Libyan coasts. However, their impact is limited in more sheltered areas, such as the Adriatic, Aegean, and Black Seas.

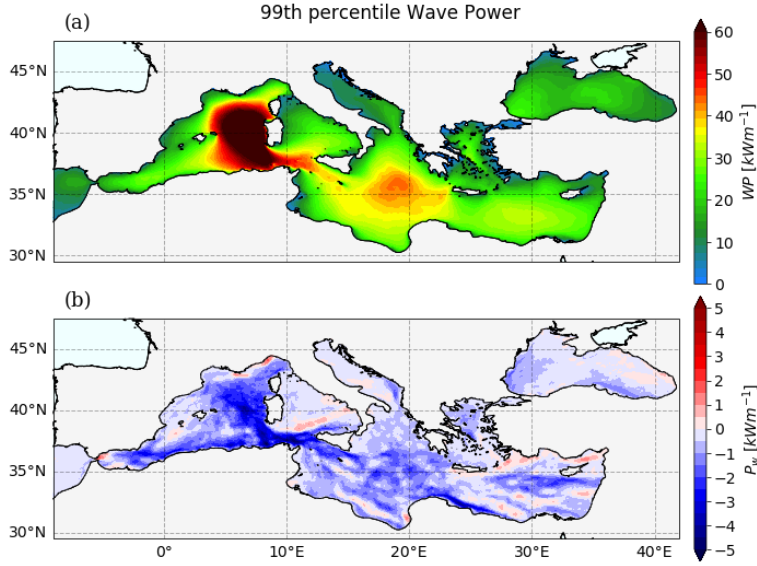


Fig. 9. (a) Yearly mean 99th percentile of wave power (kW m^{-1}) from the simulation without ocean current forcing. (b) The corresponding difference between simulations with and without current forcing. Reference period: 2020–2024.

4 Summary and discussion

We examined the spatiotemporal distribution of wave energy resources in the Mediterranean and Black Seas using a new WW3-based hindcast over a 15-year period (2010–2024), with 1-hour temporal and $1/12^\circ$ spatial resolution. To evaluate the model's accuracy, we compared ERA5 wind forcing and simulated significant wave heights with multi-mission altimeter observations. The validation results reveal a slight underestimation of significant wave heights, mainly attributed to the underestimated wind speeds in the ERA5 dataset. The biases of the selected wind forcing dataset is a well-known source of error in wave modeling (e.g., [44,45]).

The analysis identified the most energetic regions in the Mediterranean as being primarily in the western basin, particularly from the Gulf of Lion to the Algerian coast (west of Sardinia), followed by the southern Ionian Sea, and the western Levantine Sea south of Crete. In the Black Sea, the western region has the highest wave energy potential, though it remains significantly lower than in the Mediterranean. The patterns of wave power potential closely follow the seasonal cycle of significant wave height, with winter being the dominant contributor to the annual mean wave power. Additionally, regions with lower energy levels, such as the Alboran Sea, central-southern Aegean Sea, and western Black Sea show potential for WECs development due to their moderate wave power variability over time. Our findings align with previous studies [10,14], though our estimated wave power resource is lower. This discrepancy is largely due to

factors such as grid resolution, atmospheric forcing, and data assimilation techniques (as included in Oikonomou [14]), all of which play a crucial role in wave modeling.

To evaluate the impact of wave-current interactions on wave power estimation, additional simulations were conducted over a 5-year period (2020-2024) without current forcing. The results show that ocean currents generally reduce wave power potential in both basins, with extreme wave power values decreasing by up to 5 kW m^{-1} in the most energetic regions. However, in certain coastal areas, wave power increased due to current forcing. This effect may be influenced by the alignment between waves and currents (e.g., [46,47]), although further research is needed to confirm this relationship. It is important to note that the GLORYS12 reanalysis currents used to force the WW3 simulations does not include tidal effects. Future studies should address this aspect, as tide-induced modulations can significantly affect shelf-scale dynamics (e.g., [48,49]).

Future extensions of this work will primarily follow three directions. First, we aim to expand the current wave-only configuration by integrating additional model components, and developing a regional coupled ocean-atmosphere-wave system for more accurate wave power assessments, as suggested by Wu [33]. Second, we plan to enhance the wave model's horizontal resolution by implementing ultra-high-resolution nested domains in nearshore regions. Lastly, a site-scale analysis will be conducted to identify suitable deployment zones for WECs based on multiple criteria including water depths, distance from the shore, marine protected areas, socio-economic constraints, and potential joint exploitation with wind power [4].

Acknowledgments

The research work was supported by the Hellenic Foundation for Research and Innovation (HFRI) under the 4th Call for HFRI PhD Fellowships (Fellowship Number: 10793). It was also supported by computational time granted by the National Infrastructures for Research and Technology S.A. (GRNET S.A.) in the National HPC facility - ARIS - under project IDs pr015017 (BOFCOAM-2) and pr017024 (CrESM).

References

1. IPCC, 2021: Climate Change 2021: The Physical Science Basis. Contribution of Working Group I to the Sixth Assessment Report of the Intergovernmental Panel on Climate Change [Masson-Delmotte, V., P. Zhai, A. Pirani, S.L. Connors, C. Péan, S. Berger, N. Caud, Y. Chen, L. Goldfarb, M.I. Gomis, M. Huang, K. Leitzell, E. Lonnoy, J.B.R. Matthews, T.K. Maycock, T. Waterfield, O. Yelekçi, R. Yu, and B. Zhou (eds.)]. Cambridge University Press, Cambridge, United Kingdom and New York, NY, USA, In press, doi:10.1017/9781009157896
2. European Commission. (2020). An EU strategy to harness the potential of offshore renewable energy for a climate-neutral future (COM/2020/741). EUR-Lex. Retrieved from <https://eur-lex.europa.eu/legal-content/EN/TXT/?uri=CELEX:52020DC0741>
3. Pisacane G, Sannino G, Carillo A, Struglia MV and Bastianoni S.: Marine Energy Exploitation in the Mediterranean Region: Steps Forward and Challenges. *Front. Energy Res.* 6:109 (2018). doi: 10.3389/fenrg.2018.00109

4. Soukissian, T.H., Denaxa, D., Karathanasi, F., Prospathopoulos, A., Sarantakos, K., Iona, A.; Georgantas, K., Mavrakos, S. Marine Renewable Energy in the Mediterranean Sea: Status and Perspectives. *Energies*, 10, 1512 (2017) <https://doi.org/10.3390/en10101512>
5. Guillou, N., Lavidas, G., Chapalain, G. Wave Energy Resource Assessment for Exploitation—A Review. *J. Mar. Sci. Eng.*, 8, 705 (2020) <https://doi.org/10.3390/jmse8090705>
6. Dialyna, E., Tsoutsos, T. Wave Energy in the Mediterranean Sea: Resource Assessment, Deployed WECs and Prospects. *Energies*, 14, 4764 (2021). <https://doi.org/10.3390/en14164764>.
7. Pompodakis, E.E., Orfanoudakis, G.I., Katsigiannis, Y., Karapidakis, E. Techno-Economic Feasibility Analysis of an Offshore Wave Power Facility in the Aegean Sea, Greece. *Energies*, 17, 4588 (2024). <https://doi.org/10.3390/en17184588>
8. Zodiatis, G., Galanis, G., Nikolaidis, A., Kalogeris, C., Hayes, D., Georgiou, G. C., Chu, P. C., & Kallos, G. Wave energy potential in the Eastern Mediterranean Levantine Basin. An integrated 10-year study. *Renewable Energy*, 69, 311–323 (2014) <https://doi.org/10.1016/J.RENENE.2014.03.051>
9. Rusu, L. Assessment of the Wave Energy in the Black Sea Based on a 15-Year Hindcast with Data Assimilation. *Energies*, 8, 10370-10388 (2015) <https://doi.org/10.3390/en80910370>
10. Besio, G., Mentaschi, L., & Mazzino, A. Wave energy resource assessment in the Mediterranean Sea on the basis of a 35-year hindcast. *Energy*, 94, 50–63 (2016) <https://doi.org/10.1016/j.energy.2015.10.044>
11. Akpinar, A., Bingölbalı, B., & van Vledder, G. P. Long-term analysis of wave power potential in the Black Sea, based on 31-year SWAN simulations. *Ocean Engineering*, 130, 482–497 (2017). <https://doi.org/10.1016/j.oceaneng.2016.12.023>
12. Islek, F., & Yuksel, Y. Inter-comparison of long-term wave power potential in the Black Sea based on the SWAN wave model forced with two different wind fields. *Dynamics of Atmospheres and Oceans*, 93, 101192 (2021). <https://doi.org/10.1016/j.dyatmoce.2020.101192>
13. Caloiero, T., Aristodemo, F., & Ferraro, D. A. Annual and seasonal trend detection of significant wave height, energy period and wave power in the Mediterranean Sea. *Ocean Engineering*, 243, 110322 (2022). <https://doi.org/10.1016/j.oceaneng.2021.110322>
14. Oikonomou, C. L. G., Denaxa, D., & Korres, G. Unlocking the Mediterranean potential: Wave energy flux and swell contributions in a semi-enclosed sea. *Ocean Engineering*, 312, 119131 (2024). <https://doi.org/10.1016/j.oceaneng.2024.119131>
15. Emmanouil, G., Galanis, G., Kalogeris, C., Zodiatis, G., & Kallos, G. 10-year high resolution study of wind, sea waves and wave energy assessment in the Greek offshore areas. *Renewable Energy*, 90, 399–419 (2016) <https://doi.org/10.1016/j.renene.2016.01.031>
16. Lavidas, G., & Venugopal, V. A 35 year high-resolution wave atlas for nearshore energy production and economics at the Aegean Sea. *Renewable Energy*, 103, 401–417 (2017). <https://doi.org/10.1016/j.renene.2016.11.055>
17. Lavidas, G., & Venugopal, V. Wave energy resource evaluation and characterisation for the Libyan Sea. *International Journal of Marine Energy*, 18, 1–14 (2017) <https://doi.org/10.1016/j.ijome.2017.03.001>
18. Vannucchi, V., Cappietti, L. Wave Energy Assessment and Performance Estimation of State of the Art Wave Energy Converters in Italian Hotspots. *Sustainability*, 8, 1300 (2016). <https://doi.org/10.3390/su8121300>

19. Amarouche, K., Akpinar, A., Bachari, N. E. I., & Houma, F. Wave energy resource assessment along the Algerian coast based on 39-year wave hindcast. *Renewable Energy*, 153, 840–860 (2020). <https://doi.org/10.1016/j.renene.2020.02.040>
20. Carillo, A., Pisacane, G., & Struglia, M. V. Exploitation of an operative wave forecast system for energy resource assessment in the Mediterranean Sea. *Frontiers in Energy Research*, 10, 944417 (2022). <https://doi.org/10.3389/fenrg.2022.944417>
21. Kozyrakis, G. V., Spanoudaki, K., & Varouchakis, E. A. Long-term wave energy potential estimation in the Aegean and Ionian seas using dynamic downscaling and wave modelling techniques. *Applied Ocean Research*, 131, 103446 (2023) <https://doi.org/10.1016/j.apor.2022.103446>
22. Kalogeris, C., Galanis, G., Spyrou, C., Diamantis, D., Baladima, F., Koukoula, M., & Kallos, G. Assessing the European offshore wind and wave energy resource for combined exploitation. *Renewable Energy*, 101, 244–264 (2017) <https://doi.org/10.1016/j.renene.2016.08.010>
23. Rusu, L., Ganea, D., & Mereuta, E. A joint evaluation of wave and wind energy resources in the Black Sea based on 20-year hindcast information. *Energy Exploration and Exploitation*, 36(2), 335–351 (2018). <https://doi.org/10.1177/0144598717736389>
24. Ferrari, F., Besio, G., Cassola, F., & Mazzino, A. Optimized wind and wave energy resource assessment and offshore exploitability in the Mediterranean Sea. *Energy*, 190 (2020). 116447. <https://doi.org/10.1016/j.energy.2019.116447>
25. Kardakaris, K., Boufidi, I., Soukissian, T. Offshore Wind and Wave Energy Complementarity in the Greek Seas Based on ERA5 Data. *Atmosphere*, 12, 1360 (2021) <https://doi.org/10.3390/atmos12101360>
26. Rusu, L. Evaluation of the near future wave energy resources in the Black Sea under two climate scenarios. *Renewable Energy*, 142, 137–146 (2019) <https://doi.org/10.1016/j.renene.2019.04.092>
27. Aydoğan, B., Görmüş, T., Ayat, B., & Çarpar, T. Analysis of potential changes in the Black Sea wave power for the 21st century. *Renewable Energy*, 169, 512–526. (2021) <https://doi.org/10.1016/j.renene.2021.01.042>
28. Lira-Loarca, A., Ferrari, F., Mazzino, A., & Besio, G. Future wind and wave energy resources and exploitability in the Mediterranean Sea by 2100. *Applied Energy*, 302, 117492 (2021). <https://doi.org/10.1016/j.apenergy.2021.117492>
29. Simonetti, I., & Cappietti, L. Mediterranean coastal wave-climate long-term trend in climate change scenarios and effects on the optimal sizing of OWC wave energy converters. *Coastal Engineering*, 179, 104247 (2023) <https://doi.org/10.1016/j.coastaleng.2022.104247>
30. Saruwatari, A., Ingram, D. M., & Cradden, L. Wave–current interaction effects on marine energy converters. *Ocean Engineering*, 73, 106–118 (2013) <https://doi.org/10.1016/j.oceaneng.2013.09.002>
31. Webb, A., Waseda, T., & Kiyomatsu, K. A high-resolution, long-term wave resource assessment of Japan with wave–current effects. *Renewable Energy*, 161, 1341–1358 (2020). <https://doi.org/10.1016/j.renene.2020.05.030>
32. Shi, X., Li, S., Liang, B., Zhao, J., Liu, Y., & Wang, Z. Numerical study on the impact of wave-current interaction on wave energy resource assessments in Zhoushan sea area, China. *Renewable Energy*, 215, 119017 (2023) <https://doi.org/10.1016/j.renene.2023.119017>
33. Wu, L., Shao, M., Sahlée, E. Impact of Air–Wave–Sea Coupling on the Simulation of Offshore Wind and Wave Energy Potentials. *Atmosphere*, 11, 327 (2020) <https://doi.org/10.3390/atmos11040327>

34. Barbariol, F., Benetazzo, A., Carniel, S., & Sclavo, M. Improving the assessment of wave energy resources by means of coupled wave-ocean numerical modeling. *Renewable Energy*, 60, 462–471 (2013). <https://doi.org/10.1016/j.renene.2013.05.043>
35. Zodiatis, G., Galanis, G., Kallos, G. et al. The impact of sea surface currents in wave power potential modeling. *Ocean Dynamics* 65, 1547–1565 (2015) <https://doi.org/10.1007/s10236-015-0880-4>
36. WW3DG, 2019. User manual and system documentation of WAVEWATCH III® version 6.07. Tech. Note 333, NOAA/NWS/ NCEP/MMAB, College Park, MD, USA, 465 pp. + Appendices
37. Barbariol, F., Davison, S., Falcieri, F. M., Ferretti, R., Ricchi, A., Sclavo, M., & Benetazzo, A. Wind Waves in the Mediterranean Sea: An ERA5 Reanalysis Wind-Based Climatology. *Frontiers in Marine Science*, 8. (2021) <https://doi.org/10.3389/fmars.2021.760614>
38. Causio S, Federico I, Jansen E, Mentaschi L, Ciliberti SA, Coppini G and Lionello P.: The Black Sea near-past wave climate and its variability: a hindcast study. *Front. Mar. Sci.* 11:1406855 (2024). doi: 10.3389/fmars.2024.1406855
39. Karagiorgos, J., Vervatis, V., Samos, I., Flocas, H., and Sofianos, S.: Ocean-wave-atmosphere coupling effect in Medicane forecasting, *Atmos. Res.*, 304, 107418 (2024) <https://doi.org/10.1016/j.atmosres.2024.107418>
40. Hersbach, H., Bell, B., Berrisford, P., Hirahara, S., Horányi, A., Muñoz-Sabater, J., Nicolas, J., Peubey, C., Radu, R., Schepers, D., Simmons, A., Soci, C., Abdalla, S., Abellán, X., Balsamo, G., Bechtold, P., Biavati, G., Bidlot, J., Bonavita, M., ... Thépaut, J.-N. The ERA5 global reanalysis. *Quarterly Journal of the Royal Meteorological Society*, 146(730), 1999–2049 (2020). <https://doi.org/https://doi.org/10.1002/qj.3803>
41. Jean-Michel, L., Eric, G., Romain, B. B., Gilles, G., Angélique, M., Marie, D., Clément, B., Mathieu, H., Olivier, L. G., Charly, R., Tony, C., Charles-Emmanuel, T., Florent, G., Giovanni, R., Mounir, B., Yann, D., & Pierre-Yves, L. T. The Copernicus Global 1/12° Oceanic and Sea Ice GLORYS12 Reanalysis. *Frontiers in Earth Science*, 9, 698876 (2021). <https://doi.org/10.3389/feart.2021.698876>
42. CMEMS (2025). WAVE_GLO_PHY_SWH_L3_NRT_014_001: Global Ocean L3 Significant Wave Height From Nrt Satellite Measurements. [Dataset] E.U. Copernicus Marine Service Information (CMEMS. Marine Data Store (MDS). (Accessed on 01-02-2025) doi: <https://doi.org/10.48670/moi-00179>
43. Cornett, A. A global wave energy resource assessment. In *Proceedings of the 18th International Offshore and Polar Engineering Conference*, Vancouver, BC, Canada, 6–11 July 2008
44. Ardhuin, F., Bertotti, L., Bidlot, J. R., Cavalieri, L., Filippetto, V., Lefevre, J. M., & Wittmann, P. Comparison of wind and wave measurements and models in the Western Mediterranean Sea. *Ocean Engineering*, 34(3–4), 526–541 (2007) <https://doi.org/10.1016/j.oceaneng.2006.02.008>
45. Bolaños-Sánchez, R., Sanchez-Arcilla, A., & Cateura, J. Evaluation of two atmospheric models for wind–wave modelling in the NW Mediterranean. *Journal of Marine Systems*, 65(1–4), 336–353 (2007). <https://doi.org/10.1016/j.jmarsys.2005.09.014>
46. Benetazzo, A., Carniel, S., Sclavo, M., & Bergamasco, A. Wave–current interaction: Effect on the wave field in a semi-enclosed basin. *Ocean Modelling*, 70, 152–165 (2013) <https://doi.org/10.1016/j.ocemod.2012.12.009>
47. Rybalko, A., Myslenkov, S. Analysis of current influence on the wind wave parameters in the Black Sea based on SWAN simulations. *J. Ocean Eng. Mar. Energy* 9, 145–163 (2023). <https://doi.org/10.1007/s40722-022-00242-1>

48. Hashemi, M. R., & Neill, S. P. The role of tides in shelf-scale simulations of the wave energy resource. *Renewable Energy*, 69, 300–310 (2014)
<https://doi.org/https://doi.org/10.1016/j.renene.2014.03.052>
49. Karagiorgos, J., Vervatis, V., & Sofianos, S. The Impact of Tides on the Bay of Biscay Dynamics. *Journal of Marine Science and Engineering*, 8(8), 617 (2020)
<https://doi.org/10.3390/jmse8080617>